J|A|C|S
ARTICLES
Published on Web 10/03/2006

# Fine Tuning the Production of Nanosized β-Carotene Particles Using Spinning Disk Processing

Natthinee Anantachoke,[†] Mohamed Makha,*[,‡] Colin L. Raston,*[,‡] Vichai Reutrakul,[†] Nigel C. Smith,[‡] and Martin Saunders[§]

*Contribution from the School of Biomedical, Biomolecular and Chemical Sciences, University of Western Australia, 35 Stirling Highway, Crawley, Perth WA 6009 Australia, Centre of Microscopy and Microanalysis, University of Western Australia, 35 Stirling Highway, Crawley, Perth WA 600,9 Australia, and Department of Chemistry, Faculty of Science, Mahidol University, Bangkok 10400, Thailand*

Received May 31, 2006; E-mail: clraston@chem.uwa.edu.au

***Abstract:*** Nanoparticles of trans-β-carotene are accessible using spinning disk processing (SDP), by varying the reaction conditions and the choice of surfactant, macrocyclic amphiphiles, sulfonato-calix[4,5,6,8]arenes, and α,β-cyclodextrins. SDP ensures rapid mixing and fast kinetics, and nanoparticles of the carotene formed in the presence of the calixarenes are stable with respect to extraction of the carotene into an organic solvent, unlike in the presence of the cyclodextrins. Insight into the supramolecular structure of the carotene nanoparticles has also been established. The mean particle sizes (dynamic light scattering, DLS) have been optimized at 40(2) and 56(1) nm and 71.4(6) and 82(1) nm, respectively, for each sulfonato-calix[5,6 and 4,8]arene, whereas the cyclodextrins form nanoparticles with a mean diameter of 71(1) and 68.5(6) nm, respectively. ζ-Potential studies show stability of all the colloidal dispersions at pH > 4 with values below −30 mV. UV−visible spectroscopy shows a blue shift indicative of H-aggregates of the carotene within the nanoparticles. The surface area derived from BET studies is 39.12 $m^2/g$ corresponding to particles of 76.7(5) nm in diameter, in agreement with sizes obtained from DLS and TEM measurements.

## 1. Introduction

The low bioavailability of many biological active and pharmaceutical compounds relates to their limited solubility in aqueous media and thus poor absorption. Conversion of coarse particles or crystalline products into nanoparticle dispersions can overcome these problems. Commonly used methods to produce nanodispersed systems have limitations in particle size selectivity and control on morphology and composition.[1] These include the use of a mechanical milling process of coarse materials ("top-down" approach) or by precipitation or condensation of the products or adducts dissolved in various solvents, followed by subsequent removal of the solvents.[2] It is generally recognized that there is a need to develop technologies for generating nanoparticles of organic compounds to replace mechanical milling processes and other unreliable processes.[3]

Spinning disk processing (SDP) (or spinning disk reactor technology) is a paradigm in process intensification for application in both chemical transformations of molecules and in the formation of monodispersed nanoparticles within a very narrow particle size distribution.[4,5] The latter is noteworthy in the context of attempting to prepare nanoparticles of *trans*-β-carotene. Refinements in conventional solution synthesis techniques for preparing nanoparticles involves the use of surfactants, concentration control, and self-limiting formation and growth processes.[6] When these are combined with conditions promoting nucleation and the rapid extinction of reactants, the resultant techniques achieve very small particle sizes often at the cost of throughput and/or increased spread in particle size. SDP has the potential for overcoming these limitations.[4,5] SDP generates very thin (1 to 200 μm) fluid films on a rapidly rotating surface (10 to 3000 rpm), within which particle formation occurs, Figure 1. The rotation of the disk generates high centrifugal force within the liquid film enhancing the mixing and heat−mass-transfer rates.[7] SDP can be used to prepare nanoparticles of inorganic materials as well as organics and pharmaceuticals. This "bottom-up" flash nanoparticle formation proceeds via transient super-saturated solutions[5,8] which are formed through precipitation reactions or upon lowering the solubility of the substances by adding a second solvent to the molecular solution.[1] Solutions formed on the surface of the disk have short and controllable residence time

[†] Mahidol University.
[‡] School of Biomedical, Biomolecular and Chemical Sciences, University of Western Australia.
[§] Centre of Microscopy and Microanalysis, University of Western Australia.

(1) Hyeon, T. *Chem. Commun.* **2002**, 927.
(2) Horn, D.; Rieger, J. *Angew. Chem., Int. Ed.* **2001**, *40*, 4330−4361.
(3) Peters, D. *J. Mater. Chem.* **1996**, *6*, 1605−1618.
(4) Boodhoo, K. V. K.; Jachuck, R. J. J. *Green Chem.* **2000**, *4*, 235.
(5) Oxley, P.; Brechtelsbauer, C.; Ricard, F.; Lewis, N.; Ramshaw, C. *Ind. Eng. Chem. Res.* **2000**, *39*, 2175−2182.
(6) Massart, R. Magnetic fluids and processes for obtaining them. U.S. Patent 4329241, 1982.
(7) Aoune, A.; Ramshaw, C. *Int. J. Heat Mass Transfer* **1999**, *42*, 2543−2556.
(8) Brechtelsbauer, C.; Lewis, N.; Oxley, P.; Ricard, F.; Ramshaw, C. *Org. Proc. Res. Dev.* **2001**, *5*, 65−68.

10.1021/ja063545n CCC: $33.50 

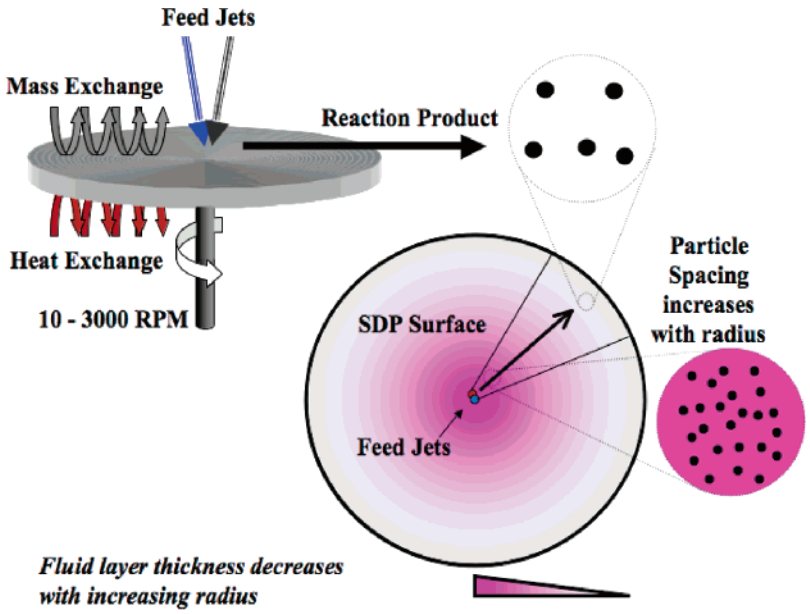


***Figure 1.*** Schematic representation of the SDP and the nucleation process taking place on the surface of the disk.

with shorter induction time for nucleation and outgrowth of the particles.[9] A key feature of SDP is the ability to control the size, size distribution, and shape of particles and surface functionality in a single pass. This has exciting possibilities in nanotechnology, especially in addressing the important issue of toxicology at the inception of the nanoscience.[10] Another feature of SDP is that it is continuous flow which facilitates scale-up and avoids the use of batch technology where there is often the need to separate mixtures.

*trans*-$\beta$-Carotene is an important bioactive organic compound or nutracuetical and is a model hydrophobic compound in studying drug nanoparticles. It is sparingly soluble in water and has poor solubility in fats and oils, and thus direct uptake of coarse particles leads to low bioavailability. The absorption of *trans*-$\beta$-carotene during the gastrointestinal process increases when the particle size is decreased, as determined by measurement of the blood-level concentrations after oral administration.[2,11] *trans*-$\beta$-Carotene dispersion hydrosols have been prepared by many techniques using a variety of stabilizers. Horn et al. reported the preparation of nanodispersed $\beta$-carotene hydrosols involving precipitation from hydrophilic solution with water in a continuous mixing chamber process[2,11] and established that the change in particle size and supramolecular structure of $\beta$-carotene particles perturbs the UV−visible absorption spectra. Hypsochromic shifts are observed for amorphous hydrosols (H-aggregate), whereas bathochromic shifts are observed for crystalline particles (J-aggregate).[11,12] Inamura et al. succeeded in solubilizing *trans*-$\beta$-carotene particles using water soluble linear polymers of PVP, PEG, PVA, and dextran.[13] There are also some reports on the formation of nanoparticles from the aggregation of $\beta$-carotene complexes with $\beta$-,$\gamma$-cyclodextrin,[14] sulfonated *p*-phenyl- and *p*-benzyl-calix[5,6]arenes,[15] which are generated by grinding methods. More recently, an emulsification−evaporation technique has been used to prepare *trans*-$\beta$-carotene nanodispersions stabilized with polyglycerol esters of fatty acids (PGEs).[16,17] In general these methods are unable to control nanoparticle size and size distributions of carotenoids while under continuous flow conditions and tend to generate larger nanoparticles than in the present study, typically >85 nm.

## 2. Results and Discussion

Herein we report the preparation and characterization of nanoparticles of *trans*-$\beta$-carotene using SDP with the particles stabilized by macrocyclic surfactants, α-, $\beta$-cyclodextrins and amphiphilic calixarenes. This highlights the utility of SDP in generating nanoparticles of an important biological molecule. A combination of various analytical techniques were used to elucidate the size and structure of carotene nanoparticles including UV−visible spectroscopy, dynamic light scattering (DLS), Brunauer−Emmett−Teller (BET) specific surface area determination, transmission electron microscopy (TEM), and X-ray diffraction. TEM imaging in particular has been used to verify the particle size and morphology characteristics, in conjunction with X-ray diffraction data for surfactant molecules, giving greater insights to the supramolecular structure of the protective layer. The SDP precipitation technique is unique in being able to control the size of the produced nanoparticles, and TEM results augment the DLS mean diameter sizing data in demonstrating low aspect ratio nanoparticles.

SDP process involves mixing the reagents as molecularly dispersed solutions on the surface of a rotating disk. Several parameters were found to affect the particle size and colloidal stability of the dispersions. Particle size decreases as the rotating disk speed increases, Figure 2a. This is consistent with increas-

(9) Cafiero, L. M.; Baffi, G.; Chianese, A.; Jachuck, R. J. J. *Ind. Eng. Chem. Res.* **2002**, *41*, 5240−5246.
(10) Albrecht, A. M. A.; Evans, C. W.; Raston, C. L. *Green Chem.* **2006**, *8*, 417−432.
(11) Horn, D. *Angew. Makromol. Chem.* **1989**, *166/167*, 139−153.
(12) Auweter, H.; Haberkorn, H.; Heckmann, W.; Horn, D.; Luddecke, E.; Rieger, J.; Weiss, H. *Angew. Chem., Int. Ed.* **1999**, *38*, 2188−2191.
(13) Inamura, I.; Isshiki, M.; Araki, T. *Bull. Chem. Soc. Jpn.* **1989**, *62*, 1671−1673.
(14) Mele, A.; Mendichi, R.; Selva, A. *Carbohydr. Res.* **1998**, *310*, 261−267.
(15) Makha, M.; McKinnon, I. R.; Raston, C. L. *J. Chem. Soc., Perkin Trans. 2*, **2002**, 1801−1806.
(16) Tan, C. P.; Nakajima, M. *Food Chem.* **2005**, *92*, 661−671.
(17) Tan, C. P.; Nakajima, M. *J. Sci. Food Agric.* **2005**, *85*, 121−126.

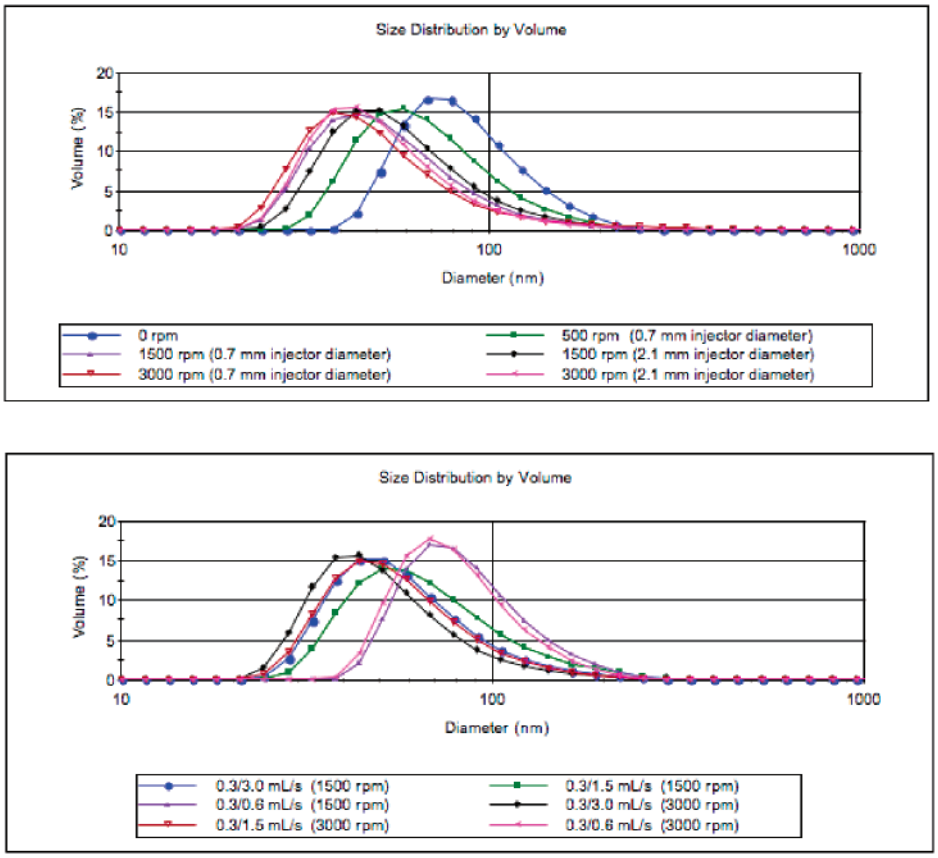


***Figure 2.*** Volume size distributions of *trans*-*β*-carotene nanoparticles dispersed in deionized Millipore water showing (a) the effect of change in speed of the spinning disk at a constant feed rate of the organic phase and aqueous phase, 0.3 and 3.0 mL/s, respectively, and (b) the effect of changing the feed rate of aqueous phase (3.0 and 1.5 mL/s using 2.1 mm feed injector diameter, 0.6 mL/s using 0.7 mm feed injector diameter) for a rotational speed of 1500 and 3000 rpm.

ing centrifugal forces under plug flow conditions.[18] Increasing the feed rate of the aqueous phase afforded smaller carotene particles as expected with limited supply of carotene particle size growth at lower concentrations (Figure 2b).

The particle size distribution depends on the feed rate of the solution, rotational speed of the disk, and head size of the feed injector with the obtained particles having Z-average diameter ranging from 70.9(7) to 129.3(7) nm. At a higher feed rate of the aqueous phase with higher disk rotation speed, the particle size has broader distribution (Figure 2b). Using a large feed injector, 2.1 mm diameter, the range of size of particles was narrow with polydispersity index (PDI) decreasing from 0.243 to 0.175 when the feed rate of the aqueous phase was 3.0 mL/s. In contrast the mean value of size of the particles was larger using a smaller feed injector (0.7 mm diameter). Here the high feed rate through the small diameter of the feed injector together with a high rotational rate leads to splashing of the solution and break down of the liquid film on the rotating disk into rivulets.[19] This results in a loss of the mixing efficiency and loss of control of particle size. However the narrow range of the particle size was observed in all of the *trans*-*β*-carotene dispersions analyzed by the PDI in the range of 0.083−0.358 (<0.5) (see Supporting Information).

Aqueous solutions of the macrocyclic oligomer (calixarenes and cyclodextrins) as surfactant resulted in particles which were resistant to extraction of the carotene into organic solvents. The mean diameter of the carotene nanoparticles prepared using pentasodium *p*-sulfonato-calix[5]arene as the surfactant was smaller than for the other calixarenes, Figure 3. The mean particle sizes (dynamic light scattering, DLS) of the carotene nanoparticles were optimized at 40(2) and 56(1) nm and 71.4-(6) and 82(1) nm, respectively, for each sulfonato-calix[5,6 and 4,8]arene, whereas the α-/*β*-cyclodextrins form nanoparticles with a mean diameter of 71(1) and 68.5(6) nm, respectively (Table 1). A surface area derived from BET studies is 39.12 $m^2/g$ corresponding to particles of 76.7(5) nm diameter, which is in agreement with DLS and TEM measurements.

***Table 1.*** Effect of Surfactant on the Size of *trans*-*β*-Carotene Nanoparticles with the Organic Phase Feed Rate at 0.3 mL/s, Aqueous Phase Feed Rate at 3.0 mL/s, and Disk Speed at 1500 rpm Using a 2.1 mm Feed Injector

| surfactant | surfactant/carotene molar ratio | PDI | Z-average (nm) | size by volume (nm) |
|---|---|---|---|---|
| $NaSO_3$calix[4]arene | 2:1 | 0.21(1) | 84(1) | 70.0(5) |
| | 4:1 | 0.20(1) | 89.7(2) | 71.4(6) |
| | 6:1 | 0.20(1) | 98.40(4) | 83(2) |
| | 8:1 | 0.19(1) | 96(1) | 80(2) |
| | 10:1 | 0.17(2) | 106(1) | 90(2) |
| $NaSO_3$calix[5]arene | 4:1 | 0.31(2) | 59(1) | 40(2) |
| $NaSO_3$calix[6]arene | 4:1 | 0.18(1) | 71.0(5) | 56(1) |
| $NaSO_3$calix[8[arene | 4:1 | 0.25(1) | 93.7(4) | 82(2) |
| $NaSO_3$calix[4,5,6,8]arenes | 4:1 | 0.21(1) | 101.1(3) | 80(1) |
| γ-cyclodextrin | 4:1 | 0.15(1) | 86.2(2) | 71(1) |
| γ-cyclodextrin | 4:1 | 0.18(1) | 87.0(6) | 68.4(6) |

(18) Leveson, P.; Dunk, W. A. E.; Jachuck, R. J. J. *J. Appl. Polym. Sci.* **2003**, *90*, 693−699
(19) Jachuck, R. J. J.; Ramshaw, C. *Heat Recovery Syst. CHP* **1994**, *14*, 475−491.

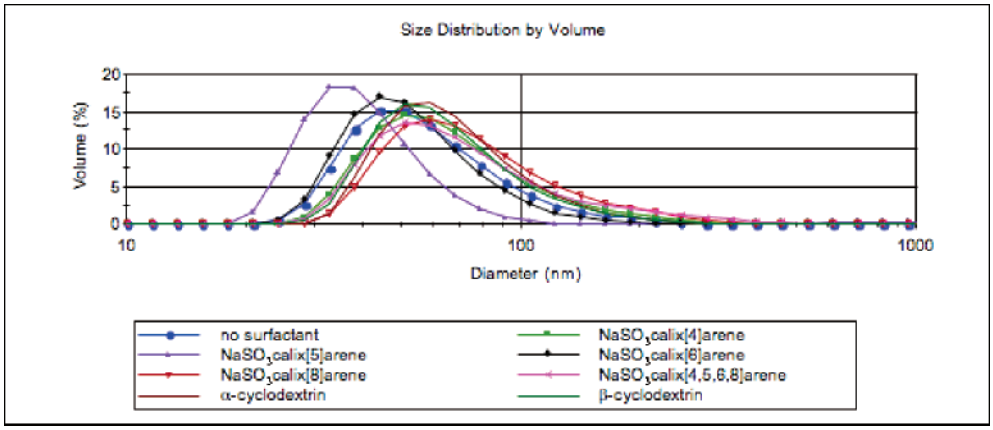


***Figure 3.*** Volume size distributions of *trans-β*-carotene nanoparticles prepared with various aqueous solutions of a macrocyclic oligomer (feed rate of organic phase to queous phase, 0.3:3.0 mL/s; feed injector diameter, 2.1 mm at 1500 rpm rotating disk speed).

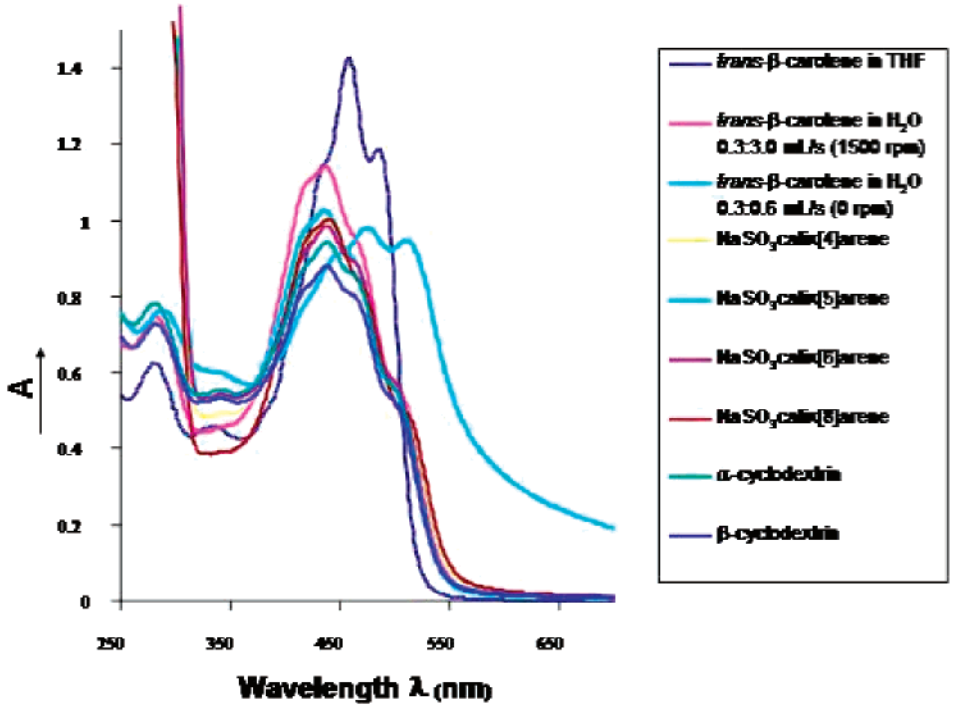


***Figure 4.*** UV−vis absorption spectra of *trans-β*-carotene dispersions showing blue shifts using feed rate of aqueous phase (with and without surfactant molecules) of 3.0 mL/s at 1500 rpm rotating disk speed (diluted 5 times with deionized water) and red shift spectrum only for the particles prepared at 0.6 mL/s feed rate of the aqueous solution at 0 rpm rotating disk speed.

Increasing the concentration of tetrasodium *p*-sulfonato-calix-[4]arene relative to the carotene resulted in larger particles as shown in Table 1. The reason for this is unclear although calixarenes themselves can form large aggregates devoid of the carotenes, which has been established from previous work.[15]

With one notable exception, hypochromic shifts of the carotene dispersions relative to molecular solutions of carotene in THF show that the carotene molecules assemble in different ways during "precipitation" forming H-type aggregates (card stack structure and amorphous solid).[12] Only one of the dispersions prepared consistently gave J-type aggregation as a fine crystalline form of *trans-β*-carotene, Figure 4. Here the feed rate of deionized water was 0.6 mL/s mixing with 0.3 mL/s of the organic solution at 0 rpm (i.e., mixing in a beaker), with the UV−vis spectrum showing a bathochromic shift of 15 nm. A hypochromic shift of 20 nm is observed when the feed rate of the aqueous solution (no surfactant present) is increased 10 fold at 1500 rpm disk speed and similar hypochromic shifts are also seen when the aqueous solutions contained a surfactant (Figure 4).

Various models for the complexation of carotene with surfactants have been proposed including aggregation of encapsulated *β*-carotene or micelle like systems.[13,15] The supramolecular interplay in the present study has been deduced from UV−vis absorption spectra and electron microscopy, Figure 5.

TEM analysis are in agreement with the DLS size distributions. Figure 6 shows typical particle morphologies for samples of *trans-β*-carotene nanoparticles produced (a) in the absence of stabilizing surfactant, (b) in the presence of sulfonato-calix-[4]arene, and (c) in the presence of sulfonato-calix[5]arene. The samples were stained with osmium tetroxide to provide enhanced contrast. Noteworthy in these TEM micrographs are the variations in stain uptake between the carotene nanoparticles. Samples produced without calixarene stabilization demonstrate

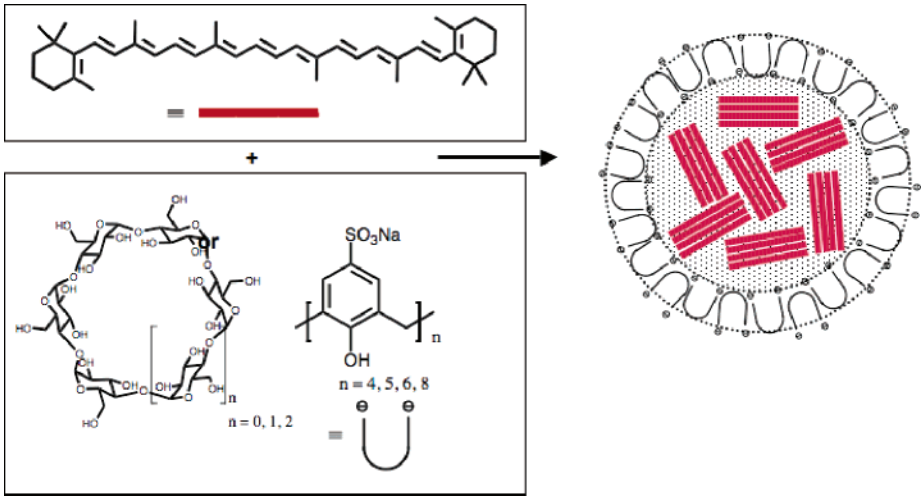


***Figure 5.*** The proposed H-aggregate model of association within the nanoparticles for the complexation of β-carotene with macrocyclic sulfonato-calix[*n*]arenes and cyclohextins.

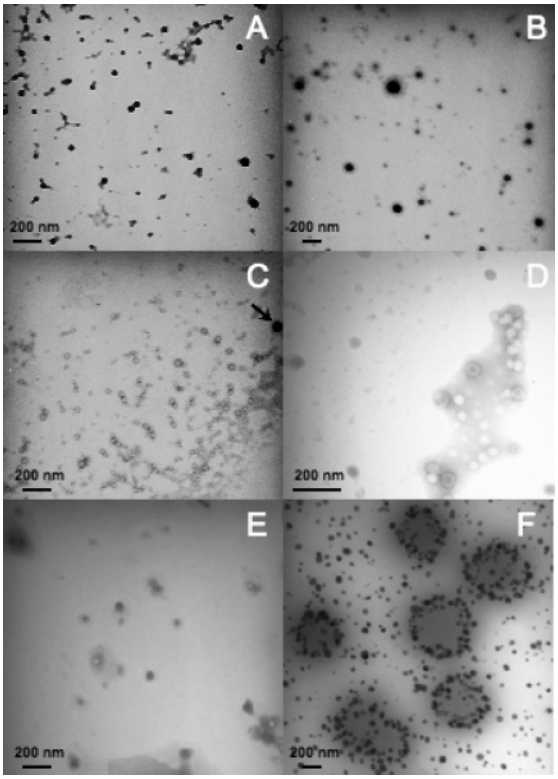


***Figure 6.*** TEM micrographs of treated β-carotene nanoparticles: (A) particles produced without stabilizer; (B) particles produced using sulfonato-calix[4]arene; (C) particles produced using sulfonato-calix[5]arene; (D) particles produced using sulfonato-calix[6] arene; (E) particles produced using sulfonato-calix[8]arene; (F) particles produced using a mixture of sulfonato-calix[4,5,6,8]arenes. Note the staining in panels A, B, E, and F is strong and throughout the particle, while in panel C the staining is only on the surface except for the indicated particle.

the typical and expected mode of staining; the particles are strongly highlighted by their adsorption and reaction of $OsO_4$ throughout the particles. Sample (c) prepared using calix[5]arene demonstrates a different staining pattern, with surface highlighting possibly arising from the binding/reaction of $OsO_4$ with the surfactant layer shrouding the carotene particles. The core of the majority of these particles is unstained, suggesting that the calix[5]arene protects the inner core in most cases.

The difference in uptake of $OsO_4$ is intriguing and potentially relates to the interplay of the calixarenes on the surface of the nanoparticles. We note that sulfonated calix[4,5, 6]arenes can form coordination polymers,[20] including complexes containing sodium, and such complexes are likely on the surface of the nanoparticles. The actual positioning of the metal ions may effect the passage of $OsO_4$ across the surface, which is restricted for most particles in the case of calix[5]arene. We also note that changing the nature of the species included in the cavity of calixarenes can dramatically effect its association with other calixarene molecules. For example, pyridine *N*-oxide in the cavity of sulfonato-calix[4]arene affords an icosahedral array of 12 calixarenes with the cavities directed away for the core of the array.[21] Incorporating 18-crown-6 in the cavities of the same calixarene as a complex of praseodymium(III) also results in a spheroidal array of 12 calixarenes albeit now as a cuboctahedral array with channels on the surface of the array connecting its interior with the surroundings.[22] This then provides a possible explanation for the variations observed in the movement of $OsO_4$ across the outer calixarene layer in some systems.

The special case of calix[5]arene affording particles mostly stable toward $OsO_4$ attack suggests that packing of 5-fold symmetry calixarenes provides a tightly assembled ordered protective outer layer. Packing of 5-fold molecules is efficient in the case of forming icosahedra, but the size of the calixarene molecules relative to the size of the particles implies that for the nanoparticles it is essentially the packing of the calixarenes on a flat surface. The formation of bilayers or higher order layers of calixarenes on the surface of the nanoparticles cannot be ruled out. All the calixarenes in the present study can form bilayers.[20]

Energy-filtered TEM imaging has permitted direct visualization of the nanoparticles without the use of osmium staining (Figure 7). Carbon elemental maps, obtained using a conventional three-window approach with a postcolumn energy filter,

(20) Atwood, J. L.; Barbour, L. J.; Hardie, M. J.; Raston, C. L. *Coord. Chem. Rev.* **2001**, *222*, 3−32. Dalgarno, S. J.; Hardie, M. J.; Raston, C. L. *Chem. Commun.* **2004**, 2802−2803. Dalgarno, S. J.; Hardie, M. J.; Atwood, J. L.; Raston, C. L. *Inorg. Chem.* **2004**, *43*, 6351−6356. Dalgarno, S. J.; Hardie, M. J.; Warren, J. E.; Raston, C. L. *J. Chem. Soc. Dalton Trans.* **2004**, 2413−2416.
(21) Orr, G. W.; Barbour, L. J.; Atwood, J. L. *Science* **1999**, *285*, 1049−1052.
(22) Atwood, J. L.; Barbour, L. J.; Dalgarno, S. J.; Hardie, M. J.; Raston, C. L.; Webb, H. R. *J. Am. Chem. Soc.* **2004**, *126*, 13170−13171.

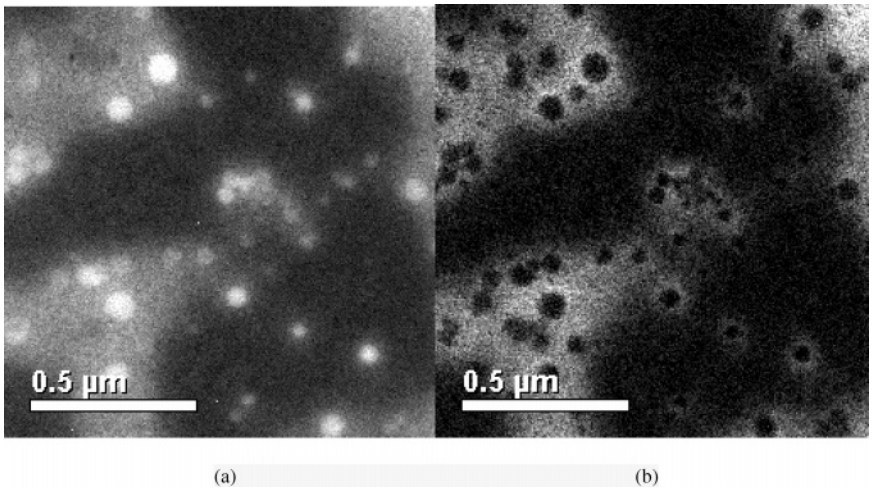


***Figure 7.*** Carbon and sulfur elemental maps of unstained $\beta$-carotene nanoparticles produced using sulfonato-calix[4]arene.

show the *trans*-$\beta$-carotene nanoparticles as bright spheres surrounded by an excess of the calixarene (Figure 7a). The corresponding sulfur map (Figure 7b) highlights the encapsulating sulfonato-calixarene, while confirming that little, if any, of the calixarene is contained within the $\beta$-carotene core, and thus the calixarene is acting as a surfactant. Particle size data obtained from these carbon maps support that obtained from the stained samples.

## 3. Conclusion

We have established the ability to control the size of *trans*-$\beta$-carotene nanoparticles using SDP down to 40 nm, with the particles stabilized by macromolecular surfactants. Essentially SDP allows the tuning of particle size formation, in the present study as spheroidal particles. This sets the scene for using the technology for preparing nanoparticles of other biologically important compounds and then using the nanoparticles for application in drug delivery systems, nutraceuticals, functional foods, and more.

## Experimental Section

*trans*-$\beta$-Carotene (95%) was supplied by Aldrich, and $\alpha$-cyclodextrin (>98%) and $\beta$-cyclodextrin (>99%) were obtained from Fluka. Tetrahydrofuran (UNICHROM) for HPLC studies was purchased from Ajax Finechem. Deionized water was used throughout the study. The sodium salts of *p*-sulfonato-calix[4,5,6,8]arenes were prepared following literature procedures.[23,24]

The SDP facility (Protensive) was manufactured from 316 stainless steel with PTFE composite seals, 100 mm disk diameter, grooved rotating disk surface, disk speed display from 300 to 3000 rpm, rate of pump flow vary from 0.3 to 3.5 mL/s. Dispersions were analyzed for mean particle diameter size and $\zeta$-potential using dynamic light scattering (Zetasizer Nano ZS series; Malvern Instruments) with 532 nm laser wavelength and a measurement angle of 173° (backscatter detection) at 25 °C. TEM analysis was carried out on a Philips 410 biological transmission electron microscope and JEOL 3000F FEGTEM equipped with a Gatan image filter. Aqueous dispersions of particles were dried in vacuo onto continuous carbon coated copper support grids and then stained by exposure to osmium tetroxide vapor for 25 min.

**Preparation of Nanoparticles of *trans*-$\beta$-Carotene using SDP. Effects of the *trans*-$\beta$-Carotene Content and Spinning Rate Relative to the Particle Size.** The carotene (0.2%w/v; 3.725 mM) was dissolved in THF. This solution was pumped at 0.3 mL/s flow rate and mixed with the aqueous phase (deionized water) onto the center of a rotating disk. The feed rates of the water were varied at 0.6, 1.5, and 3.0 mL/s in order to study the affect of the content of the carotene on particle size. The speed of the disk was adjusted by using a control regulator between 500 and 3000 rpm. Samples were collected and volatiles were removed using a reduce pressure rotary evaporator.

**Effects of the Different Macrocyclic Oligomers on Particle Size.** Aqueous solutions of $\alpha$-, $\beta$-cyclodextrin and sodium salts of *p*-sulfonato-calix[4, 5, 6 and 8] arenes (1.490 mM; 4 mole ratio to the carotene in the dispersion) were fed onto the 1500 rpm spinning disk with a flow rate of 3.0 mL/s simultaneously with an organic solution of the carotene at the same flow rate.

**Effect of the Concentration of the Macrocyclic Oligomers on Particle Size.** Concentrations of aqueous solutions of *tetra*-sodium *p*-sulfonato-calix[4]arene were varied from 2 to 10 mole ratio of the calixarene relative to the carotene.

Volatiles in the dispersions of the carotene collected from the SDP were removed under vaccuo, and the resulting aqueous solution were filtered using standard filter paper (Whatman Grade 1:11 mm). The dispersions were then analyzed for mean particle diameter size and $\zeta$-potential using DLS. The particle size is described by volume distribution and calculated in the terms of hydrodynamic diameter $d$(H) by the Stokes−Einstein equation.[25]

Particle size distributions were analyzed by a polydispersity index (PDI) as a measure for the width of the distributions with PDI values above 0.5 being indicative of a broad distribution.

The effect of pH and ionic strength on the stability of the dispersions were investigated with the pH adjusted using 0.1 M aqueous NaOH and HCl. Sodium chloride was used as to vary the ionic strengths (0.0001, 0.001, 0.003, 0.005, 0.01, 0.05, 0.1 M). All of the measurements were carried out at a temperature of 25 °C. $\zeta$-Potential is related to the electrophoretic mobility by the Henry equation.[26]

The supramolecular structure of the particles were elucidated using UV−vis absorption spectroscopy. Samples were diluted with deionized water and the spectra compared to that of trans-$\beta$-carotene in THF ($2.5 \times 10^{-3}$%w/v).

(23) Gutsche, C. D.; Dhawan, B.; Leonis, M.; Stewart, D. R. *Org. Synth.* **1989**, *68*, 238. Stewart, D. R.; Gutsche, C. D. *Org. Prep. Proc. Int.* **1993**, *25*, 137. Makha, M.; Raston, C. L.; Skelton, B. W.; White, A. H. *Green Chem.* **2004**, *6*, 158−160.

(24) Shinkai, S.; Mori, S.; Koreishi, H.; Tsubaki, T.; Manabe, O. *J. Am. Chem. Soc.* **1986**, *108*, 2409. Makha, M.; Raston, C. L. *Chem. Commun.* **2001**, *23*, 2470; Makha, M.; Raston, C. L. *Tetrahedron Lett.* **2001**, 6215.

(25) $d$(H) = $kT/3\pi hD$: see Bowen, W. R.; Mongruel, A. *Colloid Surf. A* **1998**, *138*, 161−172.

(26) $U_E = 2\varepsilon z f(\kappa a)/3\eta$: see Chibowski, E.; Wiacek, A. E.; Holysz, L.; Terpilowski, K. *Langmuir* **2005**, *21* (10), 4347−4355.

**Acknowledgment.** We are grateful for support of this work by the Australian Research Council and Protensive-UK. The microscopy analysis was carried out using facilities at the Centre for Microscopy and Microanalysis, The University of Western Australia, which are supported by University, State and Federal Government funding. The award of a senior research scholar to Prof. V. Reutrakul by the Thailand Research Fund and the financial support from the university development commission, and The Commission of Higher Education and PERCH are gratefully acknowledged.

**Supporting Information Available:** Data on the SDP reaction conditions and additional graphs for dynamic light scattering and ζ-potential measurements are included as well as experimental details. This material is available free of charge via the Internet at http://pubs.acs.org.

JA063545N